

Identification of the common regulators for hepatocellular carcinoma induced by hepatitis B virus X antigen in a mouse model

Jeng-Wei Lu^{1,2,†}, Yu Hsia^{1,†}, Wan-Yu Yang¹, Yu-I Lin¹,
Chao-Chin Li³, Ting-Fen Tsai^{1,3}, Ko-Wei Chang⁴,
Grace S. Shieh⁴, Shih-Feng Tsai¹, Horng-Dar Wang⁵ and
Chiou-Hwa Yuh^{1,6,7,*}

¹Institute of Molecular and Genomic Medicine, National Health Research Institutes, Taiwan, ²Department of Life Sciences, National Central University, Taiwan, ³Department of Life Sciences and Institute of Genome Sciences, National Yang-Ming University, Taiwan, ⁴Institute of Statistical Science, Academia Sinica, Taiwan, ⁵Department of Life Science and Institute of Biotechnology, National Tsing-Hua University, Taiwan, ⁶College of Life Science and Institute of Bioinformatics and Structural Biology, National Tsing-Hua University, Taiwan and ⁷Department of Biological Science and Technology, National Chiao Tung University, Taiwan

*To whom correspondence should be addressed. Institute of Molecular and Genomic Medicine, National Health Research Institutes, R2-3033, #35 Keyan Road, Zhunan Town, Miaoli County 350, Taiwan, ROC. Tel: +886 37 246166 35338; Fax: +886 37 586459; Email: chyuh@nhri.org.tw

Hepatitis B virus X antigen plays an important role in the development of human hepatocellular carcinoma (HCC). The key regulators controlling the temporal downstream gene expression for HCC progression remains unknown. In this study, we took advantage of systems biology approach and analyzed the microarray data of the HBx transgenic mouse as a screening process to identify the differentially expressed genes and applied the software Pathway Studio to identify potential pathways and regulators involved in HCC. Using subnetwork enrichment analysis, we identified five common regulator genes: *EDN1*, *BMP7*, *BMP4*, *SPIB* and *SRC*. Upregulation of the common regulators was validated in the other independent HBx transgenic mouse lines. Furthermore, we verified the correlation of their RNA expression levels by using the human HCC samples, and their protein levels by using the human liver disease tissue arrays. *EDN1*, bone morphogenetic protein (BMP) 4 and *BMP7* were up-regulated in cirrhosis, *BMP4*, *BMP7* and *SRC* were further up-regulated in hepatocellular or cholangiocellular carcinoma samples. The trend of increasing expression of the common regulators correlates well with the progression of human liver cancer. Overexpression of the common regulators increases the cell viability, promotes migration and invasiveness and enhances the colony formation ability in Hep3B cells. Our approach allows us to identify the critical genes in hepatocarcinogenesis in an HBx-induced mouse model. The validation of the gene expressions in the liver cancer of human patients and their cellular function assays suggests that the identified common regulators may serve as useful molecular targets for the early-stage diagnosis or therapy for HCC.

Introduction

Hepatocellular carcinoma (HCC) is the major histological type of primary liver cancer worldwide (1,2), and viral infection [hepatitis B virus (HBV) or hepatitis C virus (HCV)] is the primary risk factor in >80% of cases (3,4). Chronic HBV infection is a major etiological factor in HCC (5), possibly through triggering specific oncogenic pathways and causing

an accumulation of genetic and epigenetic alterations in regulatory genes (6–8). Although HBV infection is recognized as playing an important role in hepatocarcinogenesis, the underlying molecular mechanisms remain unknown.

Hepatitis B virus X antigen (HBx), a protein of 154 amino acids, could cause enhanced colony formation or transformation of cells *in vitro* in various cell lines (9–11). HBx has been shown to activate gene expression via oncogenic Ras signaling by increasing TATA-binding protein levels (12–14). Several HBx transgenic mouse models that develop HCC have also been created (15–17). Recently, transgenic mice model in which the albumin promoter drives the expression of HBx were shown to develop HCC at ~14 to 16 months without chemical treatment (15,18). This HBx-induced HCC mouse model has proven to be powerful for identifying potential chemopreventive agents of HBV-related hepatocarcinogenesis (18).

Several microarray-based studies have been done to identify the disease genes involved in carcinogenesis (19–22). Gene expression profiling of human liver cancer cells yielded evidence that HBx regulates many genes that may be involved in HCC (11). No study has yet been reported to identify the early-stage regulators that control the temporal gene expression of several downstream genes, which may contribute to HCC formation. Systems biology provides the means to identify the common regulators in the spatial and temporal regulation of a specific biological function. The common regulators are defined to be the key genes (like commanders) that control the temporal expression of the downstream oncogenes and tumor suppressor genes differentially expressed during different cancer formation stages. The expressions of the common regulators occur earlier than their target genes, thus to regulate the expression of those downstream target genes. Therefore, the identification of the common regulators at the early stage might be a more effective switch to pause the systematically biological functions.

In this study, we applied systems biology approach to analyze the microarray data from the whole genomic expression profile of the liver at the different time points of HBx transgenic mouse, which serves as a screening process to identify differentially expressed genes. Afterward, we validated the expression profile of the identified candidate regulators in four other independent HBx transgenic mouse lines and applied the software Pathway studio to identify potential pathways and regulators involved in the HCC carcinogenesis. Furthermore, we confirmed the expression profile in both RNA and proteins of the identified candidate regulator genes in human HCC samples. We found that the RNA levels of common regulators were upregulated in human HCC samples and the protein levels of *EDN1*, bone morphogenetic protein (BMP) 4 and *BMP7* were upregulated in cirrhosis, *BMP4*, *BMP7* and *SRC* were upregulated in HCC or cholangiocellular carcinoma (CC) samples and *EDN1* was upregulated in cirrhosis and inflammation liver samples and then downregulated in HCC specimens. Overexpression of those common regulators could increase the cell viability, promote migration and invasiveness and enhance the colony formation ability in Hep3B cells. Taken together, it indicates that our approach allows us to identify precancer oncogenes and cancer stage maintenance genes that might serve as potential therapeutic target molecules for HCC treatment. The identification of the common regulator genes at a stage prior to cancer formation during HCC formation may be a new means to develop the potential drug targets to not only eliminate but also if possibly prevent HCC.

Material and methods

HBx transgenic mice used for microarray analysis

Four transgenic mice lines overexpressing HBx in the liver were successfully established (15). All of the HBx transgenic mice are in the C57BL/6 inbred genetic background. For transgene copy numbers, overexpression of HBx in the transgenic livers and reproduction and growth status, please see previous

Abbreviations: BRCA1, breast cancer 1; CC, cholangiocellular carcinoma; cDNA, complementary DNA; HBV, hepatitis B virus; HCV, hepatitis C virus; HCC, hepatocellular carcinoma; IHC, immunohistochemistry; MAPK, mitogen-activated protein kinase; Q-PCR, quantitative polymerase chain reaction.

[†]These authors contributed equally to this work.

publication (15). All of the mice were housed in a specific-pathogen-free facility. All of the animal protocols were consistent with the recommendations outlined in the 'Guide for the Care and Use of Laboratory Animals' (National Academy Press, Washington, DC) and strictly follow the rules issued by Institutional Animal Care and Use Committees of the National Yang-Ming University and National Health Research Institutes.

Experimental design and microarray

To identify potential differentially expressed genes, we used one transgenic mouse for each time points (1.5, 8, 12, 14, and 16 months) for microarray analysis as a screening process. All of the mice are male and in the C57BL/6 genetic background. In 14- and 16-month-old mice, tumor and adjacent non-tumor tissues were obtained from the same lobe of the liver. For a control, RNA was isolated from liver samples obtained from age-matched wild-type C57BL/6 mice. The liver was excised from different stage HBx transgenic mice (line A106), and RNA was immediately isolated from the liver tissue. RNA samples were tested with an Agilent 2100 Bioanalyzer (Agilent Technologies, Santa Clara, CA) for purity and quantity. Fragmented complementary DNA (cDNA) was prepared (1 µg) following Roche NimbleGen's (Madison, WI) double-stranded (ds) cDNA synthesis protocol by using SuperScriptII ds cDNA synthesis kit (Invitrogen, Carlsbad, CA) followed by RNase treatment. RNA integrity, ds cDNA quality and all samples for microarray analysis passed NimbleGen quality control. A high-density DNA array prepared using Maskless Array Synthesizer technology from NimbleGen *Mus musculus* 1-Plex Array (NimbleGen design name MM8_60mer_expr, NimbleGen design ID 5045, catalog number: A4543-00-01, *Mus musculus* 385K array for 42 586 genes, nine probes per gene) was used for hybridization. Labeling, hybridization and scanning were performed by NimbleGen Systems following a standard operating protocol (see www.nimblegen.com). The raw data (.pair file) were subjected to Robust Multi-Array Analysis, quantile normalization and background correction, as implemented in the NimbleScan software package, version 2.4.27 (Roche NimbleGen). The microarray data presented in this study were approved by the Gene Expression Omnibus (series accession number GSE15251). The data were incorporated into GeneSpring 7.3 (Strand Life Sciences, San Francisco, CA; Agilent Technologies, Inc.). Per chip and per gene normalizations were applied according to GeneSpring's guidelines.

Statistical analyses

We developed a statistical method that combines 'trend analyses' and 'differential expression' to identify the presumptive oncogenes and tumor suppressor genes. Supplementary files 6 contain the information of *T*-test from late versus early stage, and Supplementary Table 7, available at *Carcinogenesis* Online, is the gene list from *T*-test of late versus early stage. Supplementary files 8 contain the information of Trend Analysis, and Supplementary Table 9, available at *Carcinogenesis* Online, is the gene list from trend analysis. The gene expression curves show expression levels during the five experimental stages: E_1 to E_5 corresponding to 1.5, 8, 12, 14 and 16 months. Based on the literature, we first obtained 415 known cancer genes (Supplementary Table 1 is available at *Carcinogenesis* Online). The Stat2 statistic was used to cluster these 415 genes according to an increasing or decreasing trend of their gene expression curves.

$$\text{Stat2} = \frac{1}{T-1} \sum_{t=1}^{T-1} \{ \sin[g_i(t+1) - g_i(t)] \times |g_i(t+1) - g_i(t)| \},$$

where $g_i(t)$ denotes the \log_2 ratio of expression of gene i in the t th experiment and $T = 5$. The Stat2 statistic measures whether there is an increasing or decreasing trend in the gene expression curve. This analysis resulted in six clusters of interest. From each cluster, we chose two to three typical genes (see 'Table of typical genes' in Supplementary Table 2, available at *Carcinogenesis* Online) to represent the trend observed in each subgroup. Owing to computer memory constraints, we excluded genes without proper names, such as xxxRik and LOCxxx and obtained a total of 18 000 genes. From this set, we selected genes that were highly correlated with at least one typical gene in each subgroup, such that their Pearson correlations (r) were >0.95 , and these genes constituted six subgroups of 'candidate genes'.

Hierarchical clustering

The expression profiles were clustered using the hierarchical clustering method with the complete linkage metric, and the clusters were visualized using Tree-View (<http://rana.lbl.gov/EisenSoftware.htm>). By the definitions of precancer and cancer subgroups, log ratios of genes from tumor samples (denoted as T) versus those from non-tumor samples (NT) should help distinguish the subgroups of precancer upregulated (or downregulated) genes from the cancer upregulated (or downregulated) genes. Therefore, the log ratios of gene expression levels at stages E_1 to E_3 , NT_4 , NT_5 , T_4 and T_5 and $\log_2(T_4/NT_4)$ and

$\log_2(T_5/NT_5)$ were used to cluster these 1940 genes, where NT_4 and NT_5 denote gene expression from non-tumor samples at stages 4 and 5 (14 and 16 months). Using hierarchical clustering with the complete linkage metric, we grouped these genes into 13 clusters. Furthermore, the majority of precancer (cancer) upregulated genes were grouped in Clusters 1 and 2 (3 and 4), whereas the majority of precancer (cancer) downregulated genes were grouped into subgroups 9 and 10 (11), respectively (Figure 2B). Hierarchical clustering was applied to log ratios of E_i/C_i , where E_i and C_i are gene expression levels of the experimental and control groups, respectively, at stage i and stages 1–5 denote 1.5, 8, 12, 14 and 16 months, respectively. Note that the experimental groups at stages 4 and 5 consist of gene expression from both tumor samples (T_4 and T_5) and non-tumor samples (NT_4 and NT_5).

RNA extraction and quantitative polymerase chain reaction

Quantitative polymerase chain reaction (Q-PCR) was used to validate the microarray results and to delineate the networks associated with carcinogenesis. We used samples from four different lines of mice, including the line examined in the microarray (line 106) and other lines. The liver was excised from 1.5-, 8-, 12-, 14- and 16-month-old male HBx transgenic mice, and RNA was isolated from the frozen liver tissue. RNA (100 µg) was reverse transcribed into cDNA using SuperScriptII ds cDNA synthesis kit (Invitrogen) followed by RNase treatment as described earlier (23). The resulting first-strand cDNA was used as template for qualitative PCR in triplicate using SYBR Green Q-PCR Master Mix Kit (Applied Biosystems, Carlsbad, CA). Oligonucleotide PCR primer pairs were designed to cross intron–exon boundaries from published sequences in the GenBank database using Primer 3 (24). Primers were purchased from Taiwanese company (Mission Biotech, Taipei, Taiwan, R.O.C.) and the oligonucleotide was column purified and salt free. The sequence of primers for Q-PCR is provided in the Supplementary Table 5, available at *Carcinogenesis* Online. The specificity of the amplification products was confirmed by size estimations on a 2% agarose gel and by analyzing their melting curves. The primer dimer was ruled out by performing no template control and analyzing their dissociation curve; without template, no cycle (C_q) values could be determined. After normalization to 18S rRNA, the expression ratio between the experimental and the control groups was calculated using the comparative $\Delta\Delta C_t$ method. For each Q-PCR, triplicates were employed and median values were calculated. At least three independent samples were used for Q-PCR, and the standard error was calculated and incorporated into the presented data as medians \pm standard errors.

Human liver cancer samples

Forty-nine human liver cancer samples with HBV positive were used in this study, in which 17 samples each were stage I or stage II, 15 samples of stage III. This study was approved by the Institutional Review Board (IRB) of National Health Research Institutes Human Ethics Committee code: EC0971102. Biosamples including tumor tissue RNA, paired non-tumor tissue RNA and related clinical HCC patient information were provided by Taiwan Liver Cancer Network (TLCN). Tumor histology was graded by an expert pathologist (Dr Huang, Shiu-Feng, National Health Research Institutes, Zhunan, Miaoli, Taiwan). Stage I refers to solitary primary tumors without vascular invasion and metastasis. Stage II refers to solitary tumors with vascular invasion or multiple tumors <5 cm. Stage III refers to multiple tumors >5 cm, tumors involving a major branch of the portal or hepatic vein or tumors with direct invasion of adjacent organs other than the gallbladder or with perforation of the visceral peritoneum. Some of the stage III patients also had regional lymph node metastasis.

Plasmid construction

Human *BMP4*, *BMP7*, *EDN1* and *SRC* cDNA was reverse transcription-PCR amplified using RNA isolated from Hep3B cells as template. The resulting PCR product was ligated into pDsRed-Monomer-Hyg-N1 (Clontech, Mountain View, CA). DNA sequence analysis confirmed the correct cDNA sequence was inserted in the vector. The primers used to amplify the cDNA are listed below. The underlined sequences are restriction enzyme cutting site used for ligation.

SalI-F-*BMP4*: GATCGTCGACATGATTCCTGGTAACCGAATG; BamHI-R-*BMP4*: GATCGGATCCCAGCGGCACCCACATCCCTC; SalI-F-*BMP7*: GATCGTCGACATGACAGTGCCTCACTGCGAGCTG; BamHI-R-*BMP7*: GATCGGATCCCAGTGGCAGCCAGGCCCGG; SalI-F-*EDN1*: GATCGTTCGACATGGATTATTTGCTCATGATTTTCTC; BamHI-R-*EDN1*: GATCGGATCCCACCAATGTGCTCGGTTGTG; XhoI-F-*SRC*: CCGCTCGAGATGGGTAGCAACAAGAGCAAGC and HindIII-R-*SRC*: CCCAAGCTTGAGGTTCTCCCCGGGCTG. Sequencing primers—DsRed-Mo-N1-F: CACCAAAATCAACGGGACTT and DsRed-Mo-N1-R: GTCTGGGTGGCCCTCGTAG.

Immunohistochemistry

Human HCC tissue microarrays were purchased from US Biomax (Rockville, MD). Four liver disease spectrum tissue microarrays (catalogue#BC03002;

US Biomax) were used: each contains 15 primary HCC, 8 CC, 8 cirrhosis of liver, 5 virus hepatitis of liver and 2 normal adjacent liver samples. The slides were deparaffinized with xylene and rehydrated by passages through decreasing concentrations of ethanol (from 100% to 70%). Endogenous peroxidase activity was blocked by 10 min incubation with citric acid buffer at 95°C. Tissue sections were then treated with 3% H₂O₂ for antigen retrieval. After rinsing in 5% fetal bovine serum for blocking, tissue sections were incubated overnight at 4°C with primary antibody. The primary antibodies used in the immunohistochemistry (IHC) are rabbit anti-BMP4 (1:100 dilution; GeneTex Inc., Hsinchu City, Taiwan, R.O.C.); mouse anti-BMP7 (Santa Cruz Biotechnology, Inc., Santa Cruz, CA 1:100 dilution); rabbit anti-Endothelin 1 (1:100 dilution; GeneTex Inc.), and rabbit anti-SRC (1:100 dilution; GeneTex Inc.). Tissue sections were washed three times in 1× phosphate-buffered saline buffer and incubated for 60 min at room temperature with goat anti-rabbit

IgG (Santa Cruz Biotechnology, Inc., at a 1:100 dilution) or goat anti-mouse IgG (Santa Cruz Biotechnology, Inc., at a 1:100 dilution). After washing in 1× phosphate-buffered saline buffer, peroxidase activity was detected by incubating tissue sections for 3–5 min at room temperature with Liquid DAB Substrate Kit (Invitrogen). Tissue sections were counterstained with Mayer's hematoxylin (Merck LTD., Taipei, Taiwan, R.O.C.). The staining intensity of BMP4, BMP7, Endothelin 1 and SRC were scored as 0 (<5%), 1 (5–25%) and 2 (25–50%) or (50–100%), respectively, according to the percentage of positively stained cells.

Cell culture, transfection, migration, cell viability [3-(4,5-dimethylthiazole-2-yl)-2,5-biphenyl tetrazolium bromide] and colony formation assays

Human Hep3B liver cancer cells were obtained from Bioresource Collection and Research Center in Taiwan and grown in Dulbecco's modified Eagle's

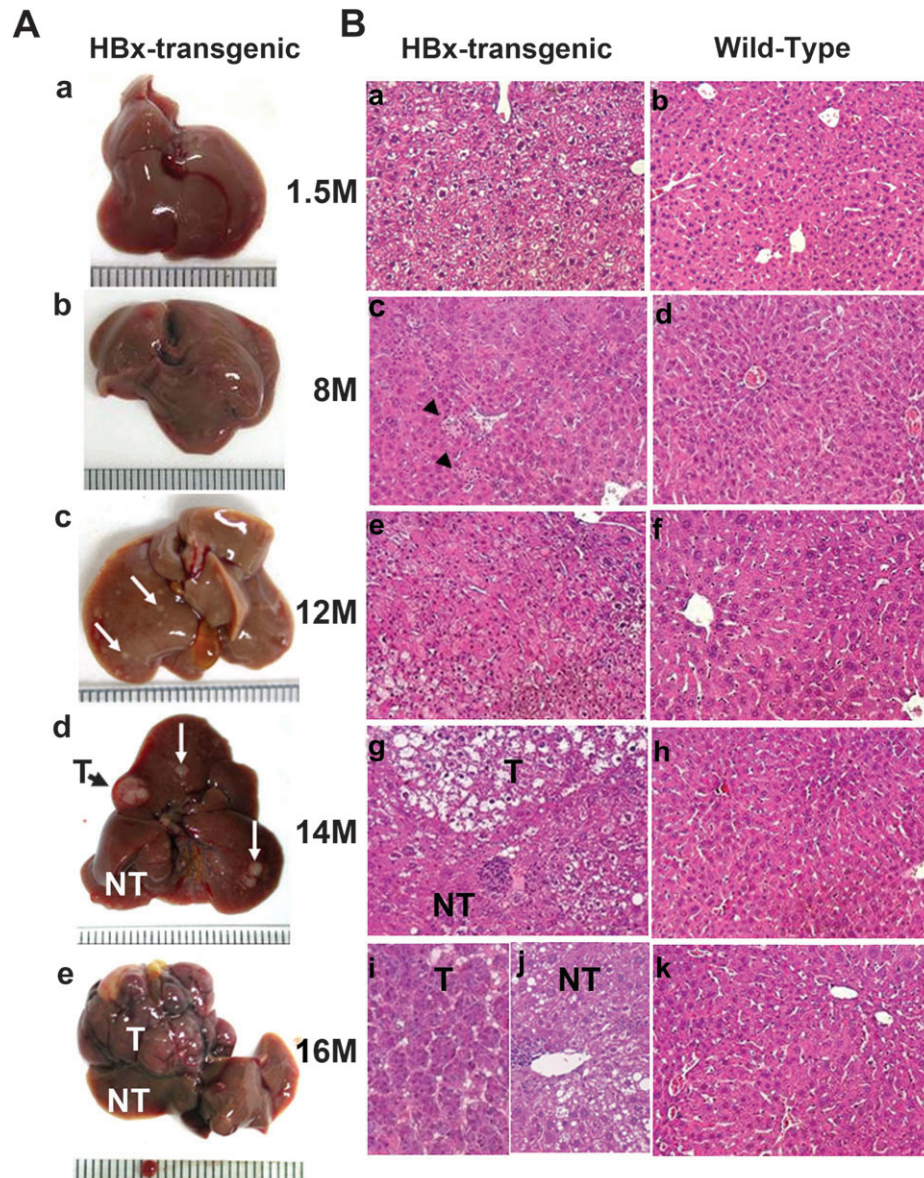


Fig. 1. Hepatocarcinogenesis in HBx transgenic mice. (A) Representative photographs of the gross liver morphology in HBx transgenic mice at different times after birth. At 1.5 (A-a) and 8 months (A-b), no overt gross morphological changes were detected. At 12 months (A-c), multiple nodules (white arrows) between 0.5 and 1.5 mm in diameter were detected. At 14 months (A-d), larger hyperplastic nodules, between 1 and 5 mm in diameter, were detected. In addition, HCC began to appear in the livers of the transgenic mice. At 16 months (A-e), an HCC incidence of ~80% was observed in the HBx transgenic mice. T, tumor; NT, non-tumor. (B) Hematoxylin and eosin stain of the liver histopathology during carcinogenesis comparing HBx transgenic mice (B-a, c, e, g, i and j) with wild-type (B-b, d, f, h and k) at different times after birth. At 1.5 months (B-a), liver degeneration, including steatosis, ballooning of the hepatocytes and abnormal arrangement of the sinusoid, were detectable in the HBx transgenic mice. However, these pathological changes largely disappeared concomitantly with quiescence of the hepatocyte cell cycle at ~2 months. At 8 months (B-c), focal necrosis and inflammation (arrow heads) were frequently observed in the transgenic livers. At 12 months (B-e), hepatic steatosis and multifocal areas of altered hepatocytes and dysplasia with mild to moderate pleomorphic nuclei were detected. At 14 months (B-g), unusual nuclei, cytoplasmic lipid droplets, necrosis, apoptosis and inflammation were frequently observed in both tumor and non-tumor tissues from the transgenic livers. At 16 months (B-i, j), pathological analysis revealed that the HCC cells were arranged in a well-differentiated trabecular pattern. Histopathology of the 16 months non-tumor tissue was similar to that obtained from 14 months mice.

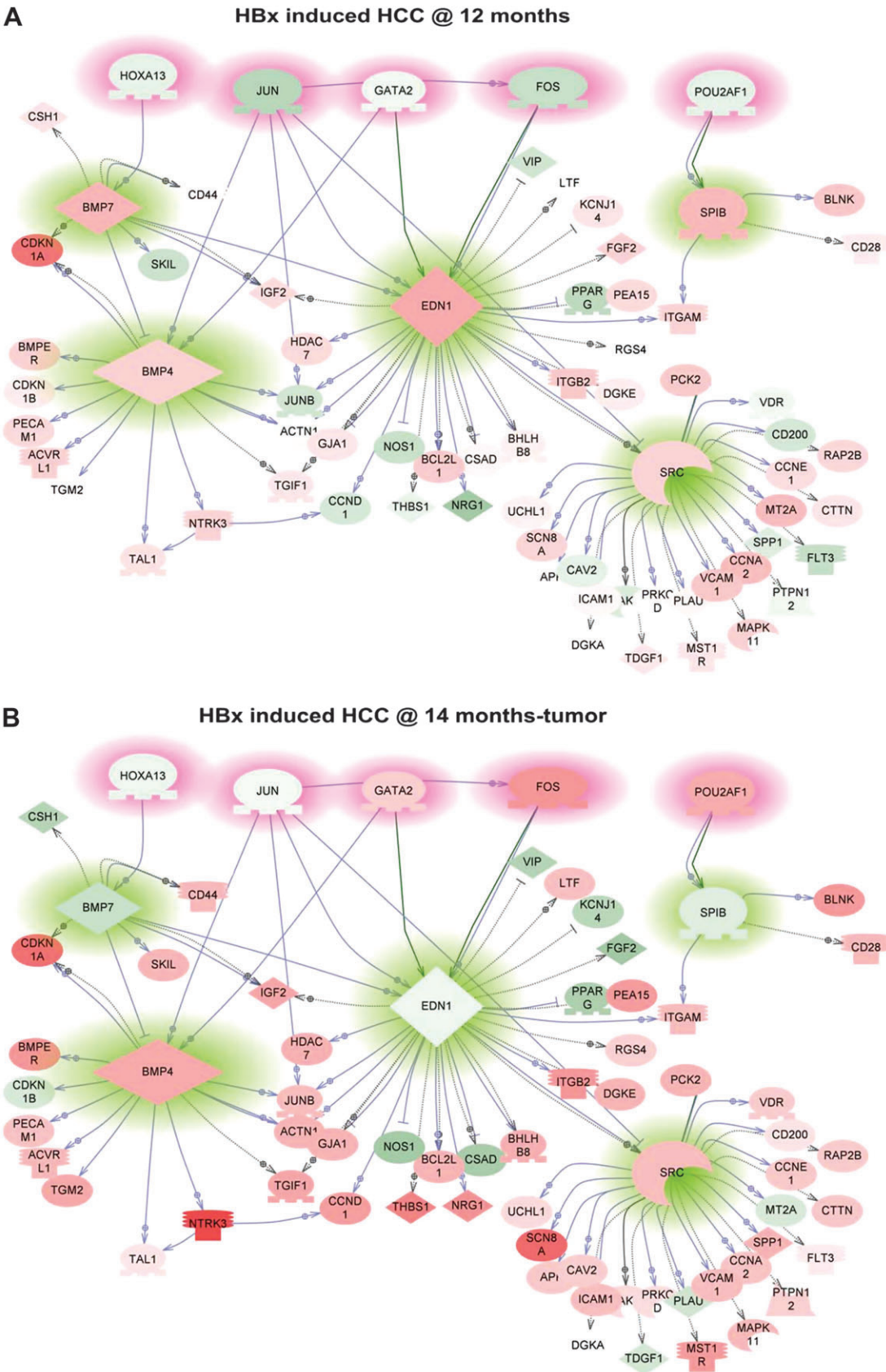


Fig. 2. Five common regulators and their downstream targets at 12 (A) and 14 months (B). The color of the genes indicates their expression level; red indicating upregulation and green indicating downregulation in HBx transgenic mice versus wild-type. The green highlighted genes are the five common regulators, whereas the pink highlighted genes are the predicted transcription factors, which had expression levels upregulated at the 8 months stage. The shapes of proteins represent the molecular functions of each gene product, either as transcription factor (with key-lock shape at the bottom), ligand (diamond shape), kinase (moon shape), receptor (T shape) or protein entity (oval shape).

medium high glucose (Gibco, Carlsbad, CA) supplemented with 10% fetal bovine serum (Gibco) and penicillin–streptomycin mixture (Gibco). Hep3B cells (530 000 cells per well) were seeded into 60 mm wells with Dulbecco's modified Eagle's medium and 10% serum. Cells were transfected with plasmid constructs encoding *BMP4*, *BMP7*, *EDN1* or *SRC* using Lipofectamine 2000 (Invitrogen). After 18 h, the cells were resuspended; half were used for Q-PCR analysis, the other half for seeding in the migration assay. After 48 h, cells on the inside of the transwell inserts were removed with a cotton swab and cells on the underside of the inserts were fixed and stained. Photographs of 10 random fields were taken, and cells were counted to calculate the average number of cells per field that had transmigrated. For 3-(4,5-dimethylthiazole-2-yl)-2,5-biphenyl tetrazolium bromide (MTT) assay, a total of 7.5×10^3 cells (100 μ l) were seeded in 96-well plates. 100 μ l of MTT (AMRESCO, Solon, OH) (MTT, stock: 5 mg/ml MTT in phosphate-buffered saline, one to dilution dilution in Dulbecco's modified Eagle's medium) was added to each well every 24 h. The plates were incubated for 4 h before addition of dimethyl sulfoxide (AMRESCO). After shocking for 10 min, the absorbance was measured at 570 nm using a microplate reader. For colony formation assay, the cells after transfected with the expression constructs encoding *EDN1* or *SRC* by using Lipofectamine 2000 (Invitrogen) were seeded at a density of 500, 1000 or 2000 cells per 60 mm well with Dulbecco's modified Eagle's medium and 10% serum. After 12 days incubation, the cells were stained with crystal violet, the resultant pictures were taken and the colonies were counted and analyzed by *t*-test.

Results

Appearance of liver, histopathological examination and HBx level in the transgenic mouse model

HBx is a known oncogenic protein encoded in HBV genome and regulates apoptosis, cell cycle, DNA repair, protein degradation and several signaling pathways (25,26). HBx transgenic mice driven by albumin promoter developed HCC at ~14–18 months (15,18). Among the independent HBx transgenic lines, A106 significantly developed HCC much faster. To understand the molecular mechanisms and identify the genes and pathways related to HBx-induced HCC, we chose A106 HBx transgenic mice to analyze the gene expression profile at different stages of HCC by using microarray.

Figure 1 represents the appearance and histopathology of the livers used in the microarray analysis. Although no obvious gross morphological changes were apparent at 1.5 and 8 months, histopathology examination showed severe degeneration at 1.5 months and focal necrosis and inflammation at 8 months in the livers of HBx transgenic mice. At 12 months, multiple small hyperplastic nodules were detected. At ~14 months of age, larger hyperplastic nodules were detected in the transgenic livers, and HCC began to appear. At ~16 months, the incidence of HCC in the HBx transgenic mice was ~80%.

We examined HBx messenger RNA at different stages in our mouse model and found that the level was ~11 and 14% at 14 and 16 months tumor samples compared with those at 1.5 months (Supplementary Figure 1 is available at *Carcinogenesis* Online). The expression level of HBx in the mouse model was similar to that observed in human HCC development, in which the HBx level is usually very low during the final stage of HCC development (27,28), see Discussion.

Potential disease genes identified by microarray analysis across HCC stages

We established genome-wide gene expression profiles during hepatocarcinogenesis in seven samples at five distinct stages (1.5, 8, 12, 14 and 16 months, both tumor and non-tumor from 14 to 16 months) with age-matched wild-type mice as control (see Materials and Methods for detail). RNA isolated from a single transgenic animal at each time point was analyzed, and all the HBx transgenic mice are in the C57BL/6 inbred genetic background. This microarray study was intended as a screen, from which we validated some of the findings in multiple independent transgenic lines. To identify as many potential disease genes for HCC as possible, two methods were used (Supplementary Figure 2A is available at *Carcinogenesis* Online). Firstly, genes with 2-fold differential expression between HBx transgenic and wild-type mice at each stage were identified by GeneSpring 7.3. Secondly, we developed a statistical method that combined trend

analyses and differential expression to identify the presumptive tumor oncogenes and suppressor genes; see Supplementary Tables 1 and 2 are available at *Carcinogenesis* Online for details. We compared the expression pattern in the early (1.5, 8 and 12 months) and late (14 and 16 months) groups because no tumor was detected at the first three stages, whereas larger hyperplastic nodules were detected in the transgenic livers at 14 months and later. If non-tumor and tumor samples had similar expression at 14 and 16 months, they were added to the precancer subgroup. On the other hand, if only tumor samples had differential expression at 14 and 16 months, they were included in the cancer subgroup. The upregulated group consisted of genes with expression levels that were not significantly different between HBx and wild-type mice at the first three stages but were increased 2-fold or more at 14 or 16 months. Conversely, the downregulated group consisted of genes that were not differentially expressed at the early three stages but were downregulated 2-fold or more at 14 or 16 months. By this process, we found 1940 genes, which were differentially expressed during hepatocarcinogenesis (data not shown). In addition to up and downregulated genes at 1.5, 8 and 12 months, there were precancer up and downregulated, cancer up and downregulated groups of genes. The expression profiles were grouped using the hierarchical clustering method with the complete linkage metric (Supplementary Figure 2B is available at *Carcinogenesis* Online). All specific groups of genes were clustered into distinct subgroups, indicating that they shared similar expression profiles and might have common functions.

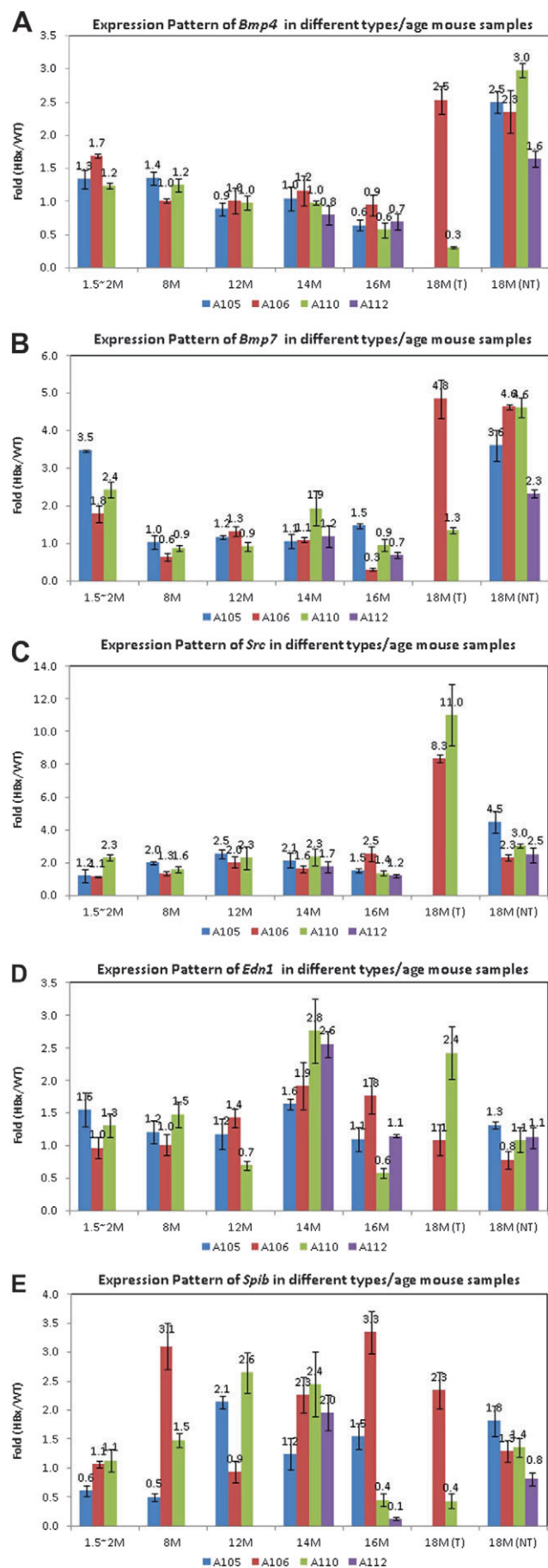
Genes involved in the non-tumor to tumor transition (12–14 months) period and their common upstream regulators

In A106 HBx transgenic mouse line, there is no cancer cells detected in the liver at the 12 months stage; however, liver cancer cells were found at the 14 months stage. It suggests that critical changes of HBx-induced HCC carcinogenesis in A106 occurred between 12 and 14 months period. To identify genes involved in this transition period, we searched for genes that exhibit 2-fold expression changes at 14 versus 12 months stage from 5775 genes that were merged from all the statistical analysis done earlier (data not shown). Next, we applied a subnetwork enrichment analysis algorithm (sNEA in Pathway Studio 6.0) to search the literatures for the potential upstream regulators. Among them, five candidate genes were found including, *Bmp4*, *Bmp7*, *Edn1*, *Spib* and *Src*, and each of the five regulates multiple downstream genes, whereas other regulators only regulate less than three downstream genes. Another criterion for selecting those five regulators is that they are significantly upregulated in 12 versus 14 months stage since a key regulator usually expresses before their target genes. Figure 2 illustrates the interactions between these five regulators (highlighted in grs are depicted in Figure 2A and 2B, in which red indicates upregulation of a gene in HBx versus wild-type and green indicates downregulation. The term of common regulators is derived from the concept of systems biology (29,30), in which the activity of differential expressed genes are controlled by common regulators. Here, five common regulators were identified in the HBx-induced HCC mouse model.

Quantitative real-time reverse transcription–PCR validation of microarray gene expression data

To confirm the expression array data, we examined RNA expression with quantitative real-time reverse transcription–PCR. RNA was isolated from liver of the line examined in the microarray (line 106) with age-matched wild-type mice as controls. We applied Q-PCR to validate the microarray data from seven samples [1.5 months, 8 months, 12 months, 14 months (T), 14 months (NT), 16 months (T) and 16 months (NT)] for 75 genes. Of these genes, 73.4% were completely identical between the microarray and Q-PCR and 17.3% matched at some stages but not all. Only 9.3% of the genes validated with Q-PCR differed from the microarray (data not shown).

The microarray results for the common regulators and their target genes were validated using Q-PCR. Three common regulators (*Bmp4*,



Bmp7 and *Edn1*) were upregulated at 12 versus 14 months tumor (Supplementary Figure 3A is available at *Carcinogenesis* Online). Both Q-PCR and microarray showed upregulation of *Bmp7* and *Edn1* at 12 months compared with 14 months tumor. Two common regulators were upregulated at 14 months tumor versus 12 months (Supplementary Figure 3B is available at *Carcinogenesis* Online). Both Q-PCR and microarray showed upregulation of *Src* at 14 months tumor compared with 12 months. Supplementary Figure 3C–G, available at *Carcinogenesis* Online, shows the expression ratio of the downstream target genes at 14 months tumor versus 12 months for those common regulators. Most of the downstream target genes that were positively regulated by the common regulators identified from the literature were indeed upregulated at 14 months according to both microarray and Q-PCR data. Three genes were predicted to be repressed by *Edn1*, but only one was downregulated at 14 months (Supplementary Figure 3F is available at *Carcinogenesis* Online). The results from 14 months non-tumor showed a similar pattern (Supplementary Figure 4 is available at *Carcinogenesis* Online), reinforcing that the transition between 12 and 14 months is a precancerous event, which occurs before final cancer formation and could be a critical juncture for hepatocarcinogenesis.

Correlation of the expression levels of the common regulators with HCC stages in the HBx transgenic mice

To evaluate the correlation between the common regulators and liver cancer, we examined the expression level for those genes from four independent lines of HBx transgenic mouse (A105, A106, A110 and A112). All four lines developed multiple nodules between 12 and 16 months, and tumors began to appear at 18 months for A106 and A110 (Supplementary Table 3 is available at *Carcinogenesis* Online). All three common regulators (*Bmp4*, *Bmp7* and *Src*) were upregulated at 18 months (Figure 3A–C). In contrast, *Edn1* expression was upregulated at 14 months (Figure 3D), and *Spib* was upregulated at many different stages (Figure 3E). Comparing the Q-PCR results and the microarray data, *Edn1* was upregulated prior to tumor formation in all four transgenic mouse lines, consistent with the line A106 used in microarray analysis. *Src* was upregulated at the tumor-forming stage in all four transgenic lines, also consistent with the A106 microarray results. However, *Bmp4* and *Bmp7* were upregulated at the tumor-forming stage in all four transgenic lines, in contrast to being upregulated at the precancer stage based on microarray data. This inconsistency might indicate multiple roles of BMPs during hepatocarcinogenesis.

The expression patterns of the identified common regulators in human HCC tissues

To check whether the identified common regulators play roles in human HCC, we examined their expression profiles in the specimens from the human liver cancer tissues compared with the normal liver biopsies of the same patients by Q-PCR. Forty-nine HBV positive (+) HCC specimens were obtained from Taiwan Liver Cancer Network (TLCN), which contain three stages (stage I, II and III) of HCC based on the classification of Tumor-lymph Nodes-Metastasis-staging system and described in Materials and Methods.

We plotted the tumor versus non-tumor ratio for the five common regulators first (Figure 4A–E) and then calculated the percentages of the HCC patients with up or downregulation of each common regulators (Figure 4F and G). *BMP4* and *SRC* were found overexpressed in most HBV (+)-HCC patients (Figure 4A, E). About 40–67% of HCC patients with >2-fold overexpression than normal control (Figure 4F). Yet there is no trend of expression changes of *BMP4* and *SRC* among the three stages of HCC. Interestingly, the expression of *EDN1* was

Fig. 3. *Bmp4*, *Bmp7*, *Src*, *Edn1* and *Spib* expression in four different transgenic mice. The expression levels of the common regulators from early to later for four lines were showed (blue for A105, red for A106, green for A110 and purple for A112). Each Q-PCR experiment was repeated more than three times, and the average result is plotted as the ratio for the expression in HBx transgenic/wild-type mice with standard deviation.

downregulated in the liver cancers of HCC patients (Figure 4C), and its lowered expression is proportional along the stage progression of HCC (Figure 4G). Furthermore, the expressions of *BMP7* and *SPIB* were all downregulated in the liver samples of HBV(+) HCC patients and their downregulation is also correlated with the stage progression of HCC. Both *SRC* and *BMP4* were upregulated as early at stage I of HCC, whereas overexpressions of *EDN1*, *BMP7* and *SPIB* may occur earlier than stage I of HCC. The data from the human liver cancers correlate to the previous findings in the livers of the HBx transgenic mice, which supports the notion that the common regulators are upregulated in precancer stage and then downregulated during cancer progression.

The protein expression levels of the common regulators in the human liver disease tissue arrays

To further examine whether the protein expression levels of these common regulators correlate to the liver disease stages throughout HCC, we performed IHC analysis of the common regulators on the tissue arrays covering the different liver disease samples from normal, inflammation, cirrhosis and malignant HCC and CC tissues. Before the IHC examination on the tissue array, we performed the pilot IHC on the tissue slices from the same HCC patients' samples for Q-PCR and proved that the data of the staining intensity from the IHC is highly correlated to the Q-PCR results (data not shown). Next, we assess the expression levels of the four common regulators by IHC on the tissue arrays for the liver diseases and HCC stages, the intensity of

IHC were classified into five scores from 0 to 4. The Supplementary Figure 5, available at *Carcinogenesis* Online, contains the representative images from the IHC to show the different levels of staining from 0 to 4. From the tissue array result, we found that the protein expressions of *EDN1*, *BMP4* and *BMP7* were upregulated in cirrhosis, *BMP4*, *BMP7* and *SRC* expressions were upregulated in the HCC or CC samples and the increase correlate to the progression of cancer (Figure 5). *EDN1* expression was upregulated in cirrhosis and inflammation liver samples and then downregulated in HCC specimens. The raw data of the tissue array are attached in the Supplementary Figure 6 and Table 4 are available at *Carcinogenesis* Online. The protein expression data of the common regulators are in accord with the RNA expression results by Q-PCR in the human liver disease samples.

Overexpressions of *BMP4*, *BMP7*, *EDN1* and *SRC* increase cell viability, enhance cell migration and promote the cell colony formation ability

To investigate the roles of the common regulators in the liver cancer cells, we overexpressed the regulator genes in Hep3B cells and performed MTT assay to test the cell viability and transwell assay to examine the migration ability. After transient transfection of the regulator genes into Hep3B cells, Q-PCR was used to measure the levels of each overexpression. We found that transient transfection effectively expresses the regulator genes in Hep3B cells with the overexpression ranging from 46.1- to 43 246.6-fold compared with the control

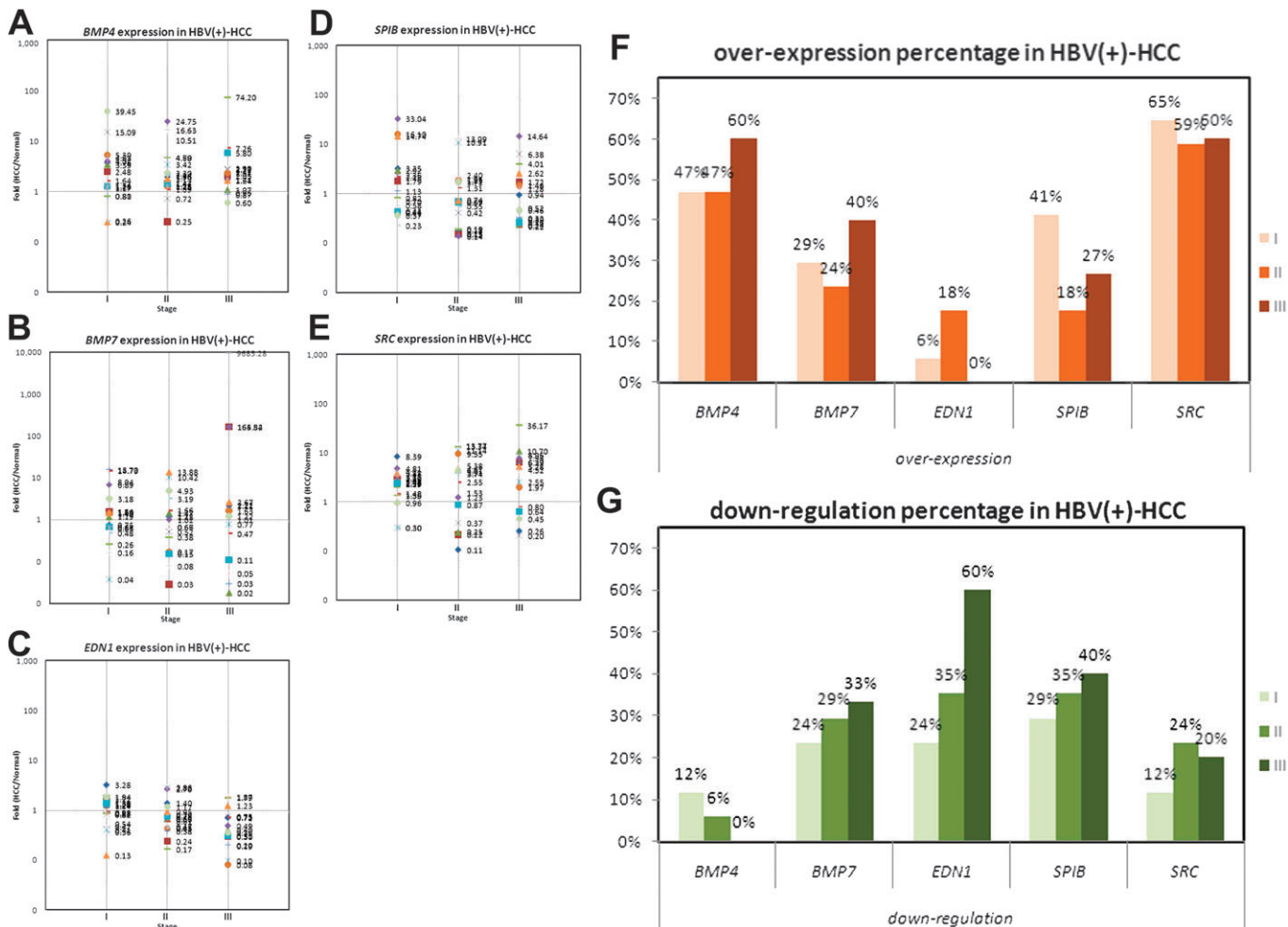


Fig. 4. *BMP4*, *BMP7*, *EDN1*, *SPIB* and *SRC* RNA expression in human HBV (+)-HCC samples. Messenger RNA expression of five common regulators in stages I, II and III was determined by Q-PCR. (A–E) The *BMP4*(A), *BMP7*(B), *EDN1*(C), *SPIB*(D), and *SRC*(E) messenger RNA expression level is calculated by normalized with 18s first and compared with the expression from adjacent non-tumor tissue. Each stage contains many patients and the expression ratios were plotted. The percentage of overexpression (F) and downregulation (G) was plotted. Orange is used to indicate overexpression, whereas green denotes the downregulation. The darker color correlates with the progress of the stage.

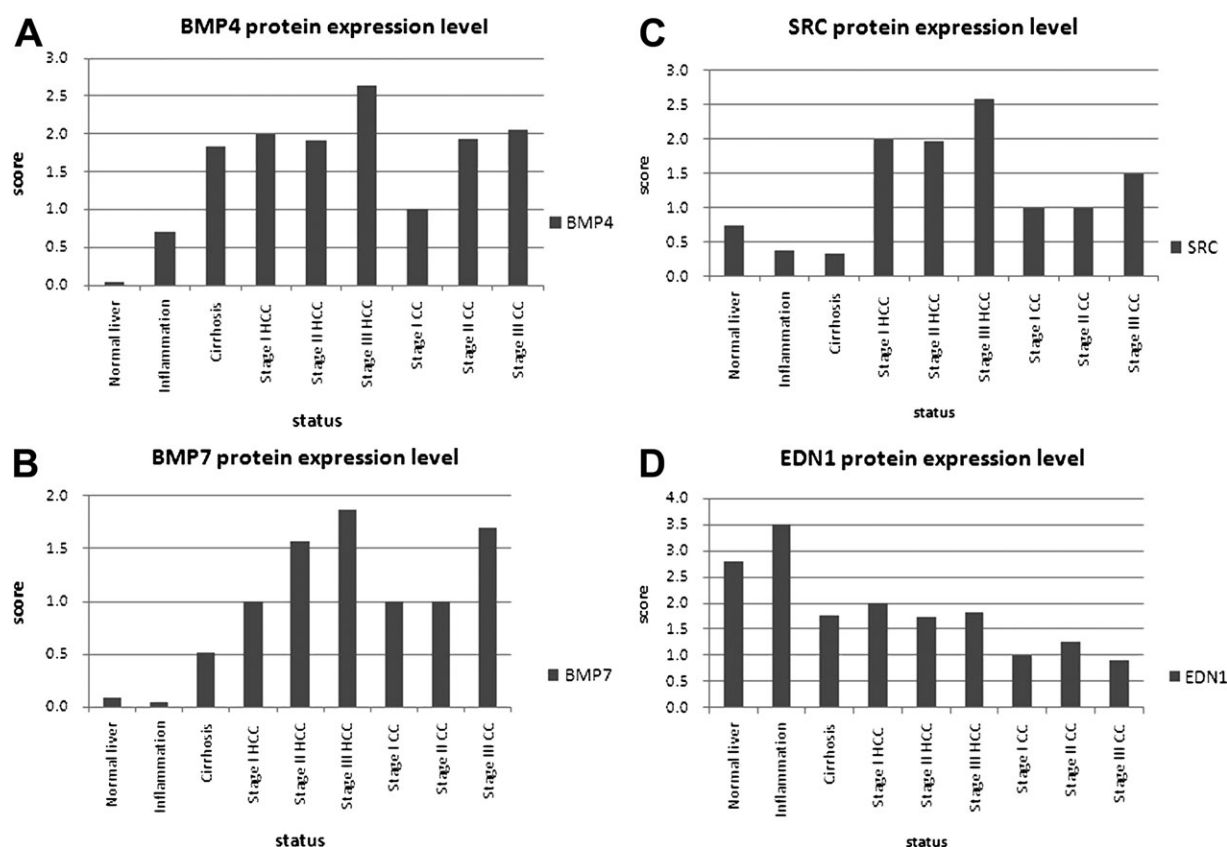


Fig. 5. BMP4, BMP7, EDN1 and SRC protein expression levels in the human liver disease spectrum tissue array. To assess the correlation between the expression of the four common regulators and the different stages of human HCC, the staining intensity of IHC were classified into five scores from 0 to 4, and the examples of each score were listed in the Supplementary Figure 7, available at *Carcinogenesis* Online. Each IHC result was evaluated and given a score and then average the scores pooled from the same stage of liver disease from the specific staining. (A) presents the score for BMP4 at different status of liver disease, (B) is for BMP7, (C) represents EDN1 and (D) illustrates the protein expression levels of SRC in different stages of liver disease.

(Figure 6A). Under MTT assay, overexpression of *BMP4* and *EDN1* dramatically increased the cell proliferation starting from the third day after transfection. On the sixth day, it increased to ~16-fold compared with the first day; however, the control only increased ~5.8-fold than the first day. Overexpression of *BMP7* and *SRC* also significantly increased the cell viability (10-fold than the first day) (Figure 6B). The transwell assay was used to detect the migration ability of the transfected Hep3B cells with each of the regulator genes. It shows that the cell migration ability increased ~2-fold compared with the control (Figure 6C). We also used colony formation assay to examine the transforming ability of overexpressing *EDN1* or *SRC* in Hep3B cells. After transient transfection of *EDN1* and *SRC* expression constructs into Hep3B cells, we seeded three different densities of the cells and let the cells grow for 12 days and then measured the total colony occupying area per plate. *SRC* overexpression can significantly increase the colonies size at the lower cell density. In the higher cell density, both *EDN1* and *SRC* dramatically enhance the colonies forming ability of the cells compare to the MOCK (Figure 6D, E). The results indicate that the properties of the *EDN1*- and *SRC*-transfected cells were changed, possibly due to activation of downstream target genes.

Discussion

HBx is regarded as a carcinogen highly related to HCC formation. However, years can elapse between HBV infection and cancer formation, implying an indirect role of HBx in activating cellular oncogenes. In the HBx transgenic mouse model, HBx induces progressive changes in the liver, tumor development correlates precisely with the binding of HBx and p53 in the cytoplasm and HBx blocks the entry of p53 into the nucleus (31). However, a direct and dose-

dependent apoptotic function of HBx independent of p53 status profoundly affected cells dying upon apoptotic stimuli *in vitro* (32) and in a transgenic mouse model (32).

Based on the HBx transgenic mouse model, the oncogenic effect of HBx is related to its expression level, specific mouse strains, type of HBx and the integration site on the genome (33). HBx under its own regulatory element causes progressive histopathological changes in the liver, beginning with multiple foci of altered hepatocytes, followed by the appearance of neoplasia (34). The high incidence of HCC (86%) in HBx transgenic mice strongly suggests that HBx plays a positive role in hepatocarcinogenesis (35). Results from these mice show that HBx promotes hepatocarcinogenesis without fibrosis (17,36), which might be due to its strong oncogenic potential (37). In some cases, HBx was unable to generate cancer by itself; its oncogenic effect required other oncogenes such as *c-myc* (38).

The level of HBx decreases as the process of hepatocarcinogenesis progresses in humans. The protein level of HBx in chronic active hepatitis, cirrhosis and HCC patients was detected in 95, 39 and 17% of patients, respectively (27). Other studies showed 30 (28,39,40) or 58.8% of HCC patients were HBx positive (41). Only one exception found a high level of HBx (84% of patients) in liver cells from patients with chronic liver disease (42). This implies HBx has multiple roles during different stages of carcinogenesis. Initially, a high level of HBx might promote apoptosis and arrest cell cycle, and individual hepatocytes with a higher level of HBx expression may undergo cell death; this might partly explain the decrease of HBx protein during hepatocarcinogenesis. Later, HBx might activate other cellular events, promoting tumorigenesis. Thus, the *in vitro* study using overexpression of HBx in cell culture might represent an early effect unrelated to HCC because of the low amount of HBx in HCC

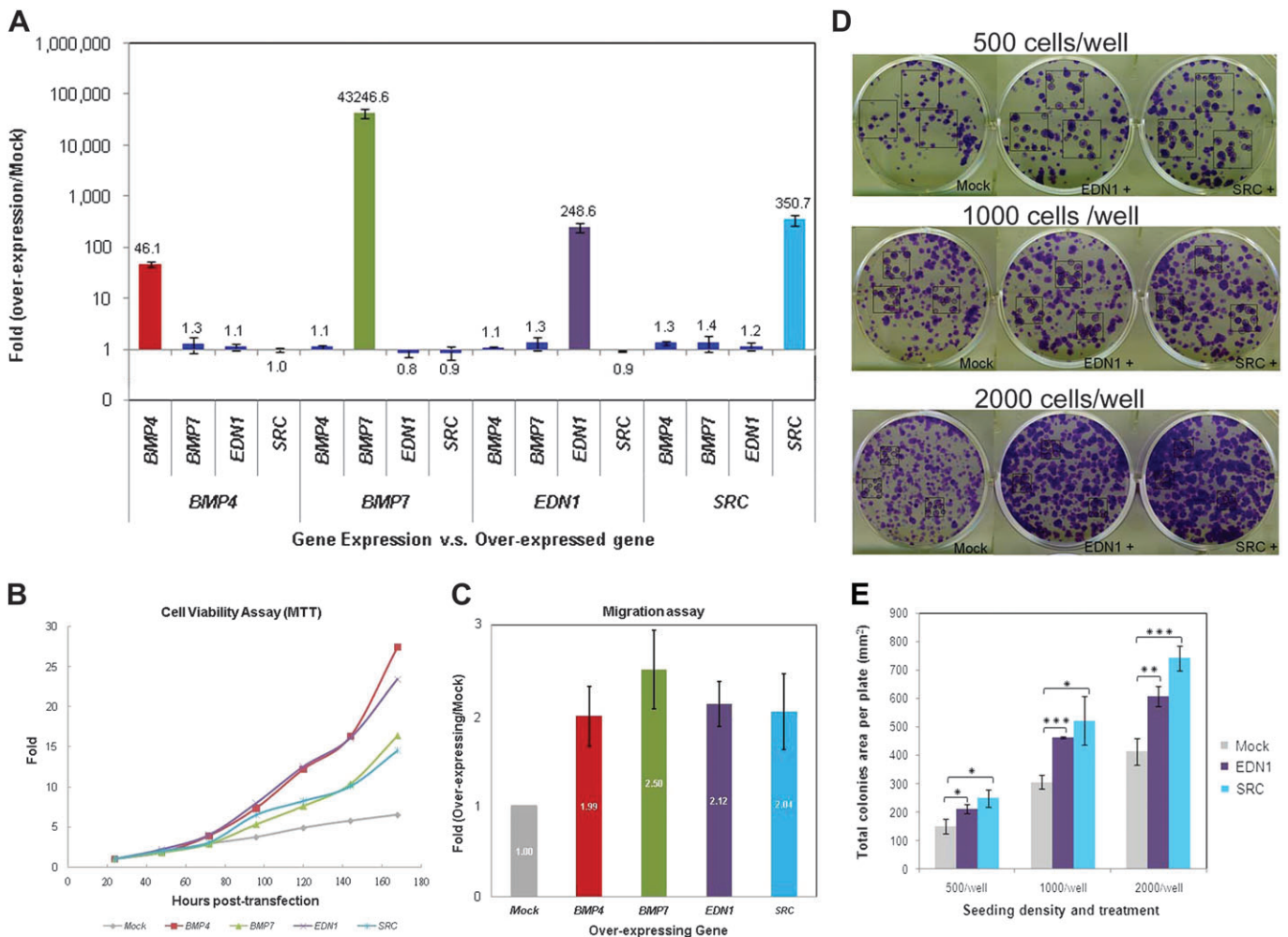


Fig. 6. Overexpressions of *BMP4*, *BMP7*, *EDN1* and *SRC* increase cell viability, migration and colony formation ability. (A) Total RNA was isolated from *BMP4*, *BMP7*, *EDN1* and *SRC* transfectants, and the expression level was examined by Q-PCR. Each Q-PCR experiment was repeated five times, and the average result is plotted as the ratio for the expression in overexpressed/mock with standard deviation. (B) Cell viability for each overexpression transfectants was measured by using MTT assay as described in the Materials and Methods. (C) Cell migration assays for each overexpression transfectants was performed by using transwell as described in the Materials and Methods. Each migration assay was repeated at least three times, and the average result is plotted as the fold difference for the number of migrated cells in overexpressed versus mock. The standard deviations from the three individual experiments were calculated and are indicated in the graph. (D) The images of the plates from the colony formation assays for MOCK, EDN1 or SRC overexpression transfectants were measured as described in the Materials and Methods. (E) Quantitative measurement of the total colonies area in different seeding density and treatments were shown. Three random fixed-size areas were chosen to count the colony occupying area and the average of the colony occupying area (mm²) is indicated with the standard deviation. T-test is used to calculate the statistical significance. **P* < 0.05, ***P* < 0.01, ****P* < 0.00.

patients. In contrast, the HBx level in our mouse model reflected human HCC; therefore, the genes and pathways identified in this mouse model might mimic human hepatocarcinogenesis.

To investigate the RNA expression profiles during different stages of HCC development, genome-wide expression arrays were performed using liver RNA obtained during early to late stages of carcinogenesis. We assessed the expression of candidate genes shown previously to be associated with HBx-induced HCC (Supplementary Table 2 is available at *Carcinogenesis* Online). Most of the genes identified previously were upregulated in the HBx-induced HCC mouse model. Both transforming growth factor-beta and the transforming growth factor-beta receptor were upregulated. Furthermore, Src tyrosine kinase (SRC: Rous sarcoma oncogene) and RAS (small G-protein, sarcoma viral oncogene)-related proteins were also upregulated, as were mitogen-activated protein kinase (MAPK)-, signal-transducer and activator of transcription protein- and Janus kinase pathway-related genes. Interestingly, these candidate genes were often upregulated during later stages of carcinogenesis (14 and/or 16 months). Conversely, the adenosine triphosphatase involved in DNA repair was downregulated

as early as 1.5 months. These findings indicate that our expression profiling data are reliable and that microarray data can be used to identify markers of HCC pathogenesis at an early stage.

The reason we used subnetwork enrichment analysis to find the common regulators for the differentially expressed genes in 14 months tumor versus 12 months was to search for the most critical genes responsible for the expression of those target genes. We actually found eight genes including MAPK3, breast cancer 1 (BRCA1) and CD44 and the five common regulators focused in this paper. However, according to literature, MAPK3, BRCA1 and CD44 upregulated many genes, which were downregulated in 14 months tumors. Also, MAPK3 only upregulated at 16 months' tumor, and both BRCA1 and CD44 are upregulated in multiple stages. Therefore, it is not possible for MAPK3, BRCA1 and CD44 be the candidate genes for the pre-cancer stage upregulated common regulators.

HBx transactivates transcription elements in the nucleus and stimulates signal transduction pathways in the cytoplasm (43,44). In the nucleus, HBx associates with CBP/p300 (C-terminal binding protein) and binds to the cAMP response element-binding elements of the

promoters of interleukin 8 and proliferating cell nuclear antigen (45). In the cytoplasm, HBx activates the protein kinase C signal pathway by elevation of Diacylglycerol (DAG), causing a significant translocation of protein kinase C to the membrane and subsequently activates activator protein 1 and other protein kinase C-dependent transcription factors such as activator protein 2 and nuclear factor-kappaB (46). HBx promotes Ras-GTP complex formation and activates the Ras/Raf/MAP kinase signaling cascade leading to activation of AP-1 and cell proliferation (47). HBx also activates the Janus kinase-signal-transducer and activator of transcription protein signaling pathway (48). Moreover, it has been demonstrated that HBx is the activator of the ATF6 and IRE1-XBP1 pathways of unfolded protein response (49). HBx may have different functions during the early or late stages of viral infection owing to its association with different transcription factors and signal transduction pathways. We have reviewed the hepatocarcinogenesis and mechanisms, which HBx caused liver cancer (8). With the advantage of a hepatocarcinogenesis animal model, we can elucidate the relationships among these pathways and genes.

Our microarray study suggested that *Bmp4*, *Bmp7*, *Edn1*, *Spib* and *Src* are critical in the 12 to 14 months transition. The proteins encoded by *Bmp4* and *Bmp7* are members of the BMP family, part of the transforming growth factor-beta superfamily. Overexpression of *Bmp4* (50) and *Bmp7* (51) has been suggested to promote migration and invasion in colon cancer. Endothelin (*Edn1*) is a 21 amino acid peptide that exerts a wide range of biological activities, and activation of the endothelin system contributes to hepatoma growth (52). *Spib* is a member of a subfamily of Ets transcription factors (53) and may be related to cancer (54), and *Src* is a kinase that may play a key role in HCC progression (55) and others have already shown that HBx activates *Src* (56). From the results, we found that upregulation of *Edn1* at the 12 months stage may trigger the expression of many downstream genes. In addition, the upregulation of *Bmp4*, *Bmp7*, *Spib* and *Src* at the 14 months stage may enhance and maintain the expression of those oncogenic genes. Overexpression of those common regulators in hepatoma cell lines further enhances cell mobility. Our study links these carcinogenetic factors to the HBx-induced HCC mouse model, establishing a possible mechanism by which liver cells become cancerous at the critical stage.

From our study, some genes critical for the transition of HCC were suggested and pathways underlying HCC formation were identified by genome-wide gene expression profiling. The relationships among early, middle and late candidate disease genes and pathways shed light on further functional analyses of HBx-induced HCC. We verified the microarray data using Q-PCR in other transgenic mouse lines and HCC patient samples. We also examined the function of overexpressing candidate genes in cell lines and observed an increase in cell mobility. Data presented here may help elucidate the molecular mechanisms involved in HBx-induced HCC in humans. However, we have to keep in mind that HBx expression in the mouse models does not necessarily reflect expression levels in the context of HBV replication and consequently, may not directly mimic what would occur in an authentic HBV infection.

Supplementary material

Supplementary Tables 1–9 and Figures 1–6 can be found at <http://carcin.oxfordjournals.org/>

Funding

National Research Program for Genomic Medicine (NSC 99-3112-B-400-010, 98-3112-B-400-003, 97-3112-B-400-008 and 96-3112-B-400-011) to C.H.Y., National Science Council (NSC) (NSC 100-2311-M-001-003-MY2, NSC-99-3112-B-001-015) to G.S.S., and NSC (97-2311-B-007-004-MY3) grant to H.D.W. are acknowledged. National Health Research Institutes to C.H.Y. TLCN is supported by grants from NSC (NSC 94-3112-B-182-002, NSC 97-3112-B-182-004) and National Health Research Institutes, Taiwan.

Acknowledgements

Funding support from National Health Research Institute to C.H.Y. is gratefully acknowledged. We would like to thank the TLCN for providing the HCC tissue samples and related clinical data (all are anonymous) for our research work. This network currently includes five major medical centers (National Taiwan University Hospital, Chang-Gung Memorial Hospital-Linko, Veteran General Hospital-Taichung, Chang-Gung Memorial Hospital-Kaohsiung and Veteran General Hospital-Kaohsiung).

Conflict of Interest Statement: None declared.

References

1. Farazi, P.A. *et al.* (2006) Hepatocellular carcinoma pathogenesis: from genes to environment. *Nat. Rev. Cancer*, **6**, 674–687.
2. El-Serag, H.B. *et al.* (2007) Hepatocellular carcinoma: epidemiology and molecular carcinogenesis. *Gastroenterology*, **132**, 2557–2576.
3. Anzola, M. (2004) Hepatocellular carcinoma: role of hepatitis B and hepatitis C viruses proteins in hepatocarcinogenesis. *J. Viral. Hepat.*, **11**, 383–393.
4. Perz, J.F. *et al.* (2006) The contributions of hepatitis B virus and hepatitis C virus infections to cirrhosis and primary liver cancer worldwide. *J. Hepatol.*, **45**, 529–538.
5. Tsai, W.L. *et al.* (2007) Molecular pathogenesis of hepatitis-B-virus-associated hepatocellular carcinoma. *Gut Liver*, **1**, 101–117.
6. Cougot, D. *et al.* (2005) HBV induced carcinogenesis. *J. Clin. Virol.*, **34** (Suppl 1), S75–S78.
7. Tsai, W.L. *et al.* (2010) Viral hepatocarcinogenesis. *Oncogene*, **29**, 2309–2324.
8. Lu, J.W. *et al.* (2011) Liver development and cancer formation in zebrafish. *Birth Defects Res. C Embryo Today*, **93**, 157–172.
9. Koike, K. *et al.* (1989) Oncogenic potential of hepatitis B virus. *Mol. Biol. Med.*, **6**, 151–160.
10. Seifer, M. *et al.* (1991) In vitro tumorigenicity of hepatitis B virus DNA and HBx protein. *J. Hepatol.*, **13** (Suppl. 4), S61–S65.
11. Zhang, W.Y. *et al.* (2009) Gene expression profiles of human liver cells mediated by hepatitis B virus X protein. *Acta Pharmacol. Sin.*, **30**, 424–434.
12. Wang, H.D. *et al.* (1995) The hepatitis B virus X protein increases the cellular level of TATA-binding protein, which mediates transactivation of RNA polymerase III genes. *Mol. Cell. Biol.*, **15**, 6720–6728.
13. Wang, H.D. *et al.* (1997) Hepatitis B virus X protein induces RNA polymerase III-dependent gene transcription and increases cellular TATA-binding protein by activating the Ras signaling pathway. *Mol. Cell. Biol.*, **17**, 6838–6846.
14. Wang, H.D. *et al.* (1998) Regulation of RNA polymerase I-dependent promoters by the hepatitis B virus X protein via activated Ras and TATA-binding protein. *Mol. Cell. Biol.*, **18**, 7086–7094.
15. Wu, B.K. *et al.* (2006) Blocking of G1/S transition and cell death in the regenerating liver of Hepatitis B virus X protein transgenic mice. *Biochem. Biophys. Res. Commun.*, **340**, 916–928.
16. Kim, C.M. *et al.* (1991) HBx gene of hepatitis B virus induces liver cancer in transgenic mice. *Nature*, **351**, 317–320.
17. Ullrich, S.J. *et al.* (1994) Transgenic mouse models of human gastric and hepatic carcinomas. *Semin. Cancer Biol.*, **5**, 61–68.
18. Wu, Y.F. *et al.* (2008) Chemopreventive effect of silymarin on liver pathology in HBV X protein transgenic mice. *Cancer Res.*, **68**, 2033–2042.
19. Yang, C.W. *et al.* (2005) Integrative genomics based identification of potential human hepatocarcinogenesis-associated cell cycle regulators: RHAMM as an example. *Biochem. Biophys. Res. Commun.*, **330**, 489–497.
20. Ng, R.K. *et al.* (2004) cDNA microarray analysis of early gene expression profiles associated with hepatitis B virus X protein-mediated hepatocarcinogenesis. *Biochem. Biophys. Res. Commun.*, **322**, 827–835.
21. Chiba, T. *et al.* (2004) Identification of genes up-regulated by histone deacetylase inhibition with cDNA microarray and exploration of epigenetic alterations on hepatoma cells. *J. Hepatol.*, **41**, 436–445.
22. Izuka, N. *et al.* (2004) Molecular signature in three types of hepatocellular carcinoma with different viral origin by oligonucleotide microarray. *Int. J. Oncol.*, **24**, 565–574.
23. Chan, T.M. *et al.* (2009) Functional analysis of the evolutionarily conserved cis-regulatory elements on the sox17 gene in zebrafish. *Dev. Biol.*, **326**, 456–470.
24. Rozen, S. *et al.* (2000) Primer3 on the WWW for general users and for biologist programmers. *Methods Mol. Biol.*, **132**, 365–386.
25. Oda, T. *et al.* (1992) p53 gene mutation spectrum in hepatocellular carcinoma. *Cancer Res.*, **52**, 6358–6364.

26. Murakami, S. (2001) Hepatitis B virus X protein: a multifunctional viral regulator. *J. Gastroenterol.*, **36**, 651–660.
27. Seo, J.H. *et al.* (1997) Lack of colocalization of HBxAg and insulin like growth factor II in the livers of patients with chronic hepatitis B, cirrhosis and hepatocellular carcinoma. *J. Korean Med. Sci.*, **12**, 523–531.
28. Pal, J. *et al.* (2001) Immunohistochemical assessment and prognostic value of hepatitis B virus X protein in chronic hepatitis and primary hepatocellular carcinomas using anti-HBxAg monoclonal antibody. *Pathol. Oncol. Res.*, **7**, 178–184.
29. Kobayashi, I. *et al.* (2010) Comparative gene expression analysis of zebrafish and mammals identifies common regulators in hematopoietic stem cells. *Blood*, **115**, e1–e9.
30. Zare, H. *et al.* (2009) Reconstruction of *Escherichia coli* transcriptional regulatory networks via regulon-based associations. *BMC Syst. Biol.*, **3**, 39.
31. Ueda, H. *et al.* (1995) Functional inactivation but not structural mutation of p53 causes liver cancer. *Nat. Genet.*, **9**, 41–47.
32. Terradillos, O. *et al.* (1998) p53-independent apoptotic effects of the hepatitis B virus HBx protein *in vivo* and *in vitro*. *Oncogene*, **17**, 2115–2123.
33. Leenders, M.W. *et al.* (2008) Mouse models in liver cancer research: a review of current literature. *World J. Gastroenterol.*, **14**, 6915–6923.
34. Koike, K. (1993) [Transgenic mouse model for hepatocellular carcinoma in human hepatitis B virus infection]. *Nippon Rinsho*, **51**, 536–541.
35. Yu, D.Y. *et al.* (1999) Incidence of hepatocellular carcinoma in transgenic mice expressing the hepatitis B virus X-protein. *J. Hepatol.*, **31**, 123–132.
36. Xu, X.B. *et al.* (2010) [Observation on experimental liver fibrosis and hepatic carcinogenesis of HBV gene knock-in transgenic mice induced by CCl₄/ethanol]. *Zhonghua Yi Xue Za Zhi*, **90**, 822–825.
37. Koike, K. (2002) Hepatocarcinogenesis in hepatitis viral infection: lessons from transgenic mouse studies. *J. Gastroenterol.*, **37** (Suppl. 13), 55–64.
38. Terradillos, O. *et al.* (1997) The hepatitis B virus X gene potentiates c-myc-induced liver oncogenesis in transgenic mice. *Oncogene*, **14**, 395–404.
39. Vitvitski-Trepo, L. *et al.* (1990) Early and frequent detection of HBxAg and/or anti-HBx in hepatitis B virus infection. *Hepatology*, **12**, 1278–1283.
40. Zentgraf, H. *et al.* (1990) Mouse monoclonal antibody directed against hepatitis B virus X protein synthesized in *Escherichia coli*: detection of reactive antigen in liver cell carcinoma and chronic hepatitis. *Oncology*, **47**, 143–148.
41. Su, Q. *et al.* (1998) Expression of hepatitis B virus X protein in HBV-infected human livers and hepatocellular carcinomas. *Hepatology*, **27**, 1109–1120.
42. Wang, W.L. *et al.* (1991) HBxAg in the liver from carrier patients with chronic hepatitis and cirrhosis. *Hepatology*, **14**, 29–37.
43. Doria, M. *et al.* (1995) The hepatitis B virus HBx protein is a dual specificity cytoplasmic activator of Ras and nuclear activator of transcription factors. *EMBO J.*, **14**, 4747–4757.
44. Caselmann, W.H. (1995) Transactivation of cellular gene expression by hepatitis B viral proteins: a possible molecular mechanism of hepatocarcinogenesis. *J. Hepatol.*, **22**, 34–37.
45. Cougot, D. *et al.* (2007) The hepatitis B virus X protein functionally interacts with CREB-binding protein/p300 in the regulation of CREB-mediated transcription. *J. Biol. Chem.*, **282**, 4277–4287.
46. Kekule, A.S. *et al.* (1993) Hepatitis B virus transactivator HBx uses a tumour promoter signalling pathway. *Nature*, **361**, 742–745.
47. Benn, J. *et al.* (1994) Hepatitis B virus HBx protein activates Ras-GTP complex formation and establishes a Ras, Raf, MAP kinase signaling cascade. *Proc. Natl Acad. Sci. USA*, **91**, 10350–10354.
48. Lee, Y.H. *et al.* (1998) HBx protein of hepatitis B virus activates Jak1-STAT signaling. *J. Biol. Chem.*, **273**, 25510–25515.
49. Li, B. *et al.* (2007) Hepatitis B virus X protein (HBx) activates ATF6 and IRE1-XBP1 pathways of unfolded protein response. *Virus Res.*, **124**, 44–49.
50. Deng, H. *et al.* (2007) Bone morphogenetic protein-4 is overexpressed in colonic adenocarcinomas and promotes migration and invasion of HCT116 cells. *Exp. Cell Res.*, **313**, 1033–1044.
51. Motoyama, K. *et al.* (2008) Clinical significance of BMP7 in human colorectal cancer. *Ann. Surg. Oncol.*, **15**, 1530–1537.
52. Pfaff, T. *et al.* (2004) The endothelin system in Morris hepatoma-7777: an endothelin receptor antagonist inhibits growth *in vitro* and *in vivo*. *Br. J. Pharmacol.*, **141**, 215–222.
53. Ray-Gallet, D. *et al.* (1995) DNA binding specificities of Spi-1/PU.1 and Spi-B transcription factors and identification of a Spi-1/Spi-B binding site in the c-fes/c-fps promoter. *Oncogene*, **11**, 303–313.
54. Muller, S. *et al.* (1996) Cell specific expression of human Bruton's agammaglobulinemia tyrosine kinase gene (Btk) is regulated by Spi-1 and Spi-1/PU.1-family members. *Oncogene*, **13**, 1955–1964.
55. Lau, G.M. *et al.* (2009) Expression of Src and FAK in hepatocellular carcinoma and the effect of Src inhibitors on hepatocellular carcinoma *in vitro*. *Dig. Dis. Sci.*, **54**, 1465–1474.
56. Klein, N.P. *et al.* (1997) Activation of Src family kinases by hepatitis B virus HBx protein and coupled signaling to Ras. *Mol. Cell. Biol.*, **17**, 6427–6436.

Received February 22, 2011; revised September 14, 2011;
accepted October 13, 2011